ORIGINAL RESEARCH

Silica nanostructures against fungal growth: design and preparation of antifungal cotton fabrics

**Ming Liu · Albert Granados · David Reyes-Mesa ·
E. Leonardo Arosemena-Angulo · María Ángeles Calvo-Torras ·
Roser Pleixats · Adelina Vallribera**

Abstract The preparation of antifungal-functionalized silica nanoparticles by covalent attachment of several silylated derivatives based on the topical antifungal agent Micozanole is described. Grafting and co-condensation procedures are used to obtain mesoporous or dense nanoparticles. Cotton fabrics have been coated with these antifungal-functionalized silica nanoparticles under ultrasonic conditions. The characterization of the functionalized nanoparticles and coated cotton fabrics is performed by microscopic and spectroscopic techniques. The antifungal activity of all the modified cotton textiles is tested against *Trichophyton mentagrophytes CECT 2783*, *Aspergillus brasiliensis CECT 2091*, *Penicillium chrysogenum CECT 2307* and *Candida albicans CECT 1001*, resulting to be highly dependent on the microorganism. Remarkably, all of the modified fabrics are active against *Candida albicans* and *Trichophyton mentagrophytes*, with up to 75 and 90% effectiveness, respectively. High expectations arise for topical cutaneous applications in wound dressings (bandages, gauzes, strips).

Albert Granados, Maria Angeles Calvo-Torras, Roser Pleixats and Adelina Vallribera are principal authors.

M. Liu · A. Granados · D. Reyes-Mesa · R. Pleixats · A. Vallribera (✉)
Departament de Química and Centro de Innovación en Química Avanzada (ORFEO-CINQA), Universitat Autònoma de Barcelona, Campus UAB, 08193 Cerdanyola del Vallès, Barcelona, Spain
e-mail: adelina.vallribera@uab.cat

M. Liu
e-mail: ming.liu@uab.cat

A. Granados
e-mail: albert.granados@uab.cat

D. Reyes-Mesa
e-mail: david.reyesm@autonoma.cat

R. Pleixats
e-mail: roser.pleixats@uab.cat

E. L. Arosemena-Angulo · M. Á. Calvo-Torras
Departament de Sanitat i Anatomia Animals, Universitat Autònoma de Barcelona, Campus UAB, 08193 Cerdanyola del Vallès, Barcelona, Spain
e-mail: arosemenaleo80@gmail.com

M. Á. Calvo-Torras
e-mail: mariangels.calvo@uab.cat

Graphical abstract
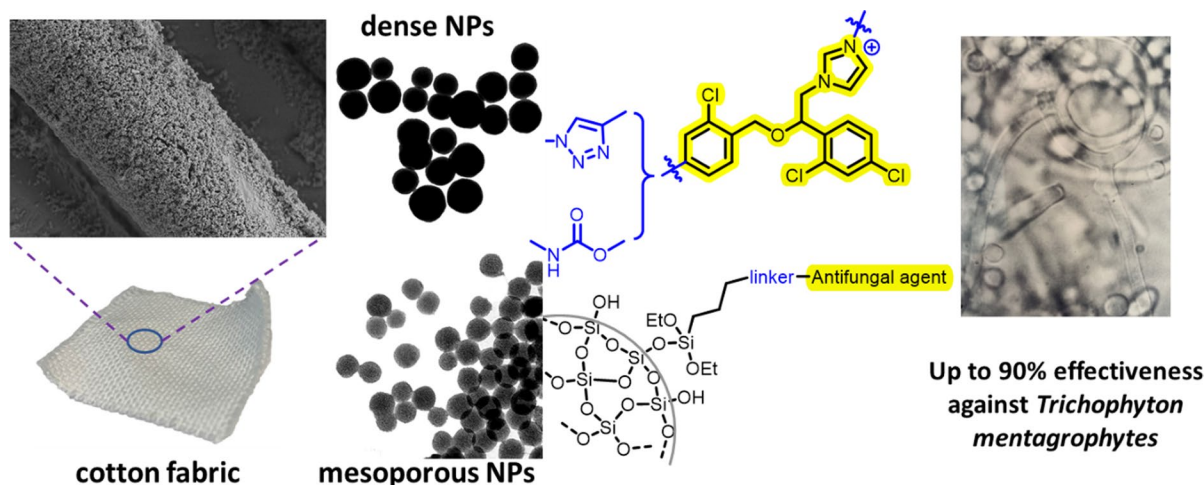
Up to 90% effectiveness against *Trichophyton mentagrophytes*

Introduction

In our daily life, it is inevitable to encounter a variety of microorganisms, which may rapidly grow and cause damage to people's health. Fungal infections represent a huge global problem resulting in over 1.7 million of deaths every year in humans and over one billion people suffer from severe fungal diseases (Brown et al. 2012). Some hosts for the fungi proliferation are food crops, animal species and textiles (Almeida et al. 2019). Focusing in the last one, textiles are excellent substrates for microbial proliferation under appropriate moisture, nutrients, and temperature conditions (Lim and Hudson 2004). In the hospital environment, contaminated cotton-based materials can infect patients and professionals. Moreover, contamination of these textiles in clinical atmospheres can contribute to the spread of airborne pathogens, which then fall by gravity and infect the environment.

Besides, in 2020 the World Health Organization developed the first meeting of the WHO antifungal expert group for the identification of priority fungal pathogens to develop a priority pathogens list for fungal infections of public health importance and to define the R&D priorities (Getahun et al. 2020). So,

this global problem has been overlooked and belittled for a long time. Additionally, in this complex scenario, global warming and accompanying climate changes have resulted in an increased incidence of many fungal diseases (Garcia-Solache and Casadevall 2010). Thus, in this context, the development of new drugs in order to treat fungal diseases is mandatory.

On the other side, cotton fabrics are widely used materials because of their excellent properties including biodegradability, softness, permeability, and hygroscope capacity. However, cotton textiles provide a good living environment for fungi because of massive hydrophilic cellulose and pores. Consequently, much effort has been done in the preparation of functional materials for avoiding the global problem of fungi proliferation on cotton surfaces.

Numerous antifungal molecular agents have been selected for coating cotton fabrics (Emam et al. 2021), including quaternary ammonium salts, *N*-halamines, recognized antifungal drugs (Ketoconazole) and bioactive dyes. Rosenau's group described the covalent grafting of xanthene-derived photosensitizers onto cellulose sheets that produce single oxygen upon white light illumination having photomicrobicidal activity (Hettegger et al. 2015a). Sun et al. synthesized derivatives of polyquaternary ammonium salts based on *N,N*-dimethylaminoethyl methacrylate which were deposited onto cotton fabrics after free radical polymerization. After a chlorine bleach the amide groups were transformed into *N*-halamines (Li et al. 2020a, b). β-Cyclodextrin with an encapsulated

antifungal drug was loaded on the surface of a wound dressing and a controlled release of Ketoconazole to skin was achieved (Hedayatia et al. 2020). Moreover, application of 1,3-bis[(furan-2-yl)methylene] thiourea (Jabar et al. 2020) and curcuma (Gargoubi et al. 2020) dyes resulted in excellent finished textiles against some fungi. The uniform dispersion of guanazole-metal complexes on cotton fabrics surface (Ag^+ and Zn^{2+}) via self-assembly resulted in antifungal and flame retardant materials (Nabipour et al. 2020).

Among the antifungal agents, several nanostructures have been intensively studied, including organic molecules-based nanoparticles (NPs), metal NPs and metal oxide NPs. An effective ultrasound assisted deposition of vanillin NPs, raspberry ketone NPs and camphor NPs on textiles was reported by Gedanken's group (Tzhayik et al. 2017). These nanomaterials were coated on cotton fabrics and showed excellent antifungal activity on cotton bandages. Recently, carbon quantum dots, nucleated from a pyrimidine-based compound or from carboxymethyl cellulose, were immobilized within a textile matrix possessing microbial inhibition (Ahmed et al. 2021; Emam et al. 2021).

Among metals, Ag NPs are the most explored. Most of the recent publications use a green route for their preparation and stabilization. It has been described the biosynthesis of Ag NPs using the corn grain contaminant (*Nigrospora oryzae*) (Dawoud et al. 2020), an endophytic actinomycete strain of *Streptomyces laurentii* previously isolated from the roots of the plant *Achillea fragrantissima* (Eid et al. 2020)*, Ulva lactuca* extracts (Sahayaraj et al. 2019), *Citrus sinensis* peel juice (AnwarKhalid and Alghamdi 2020), *Moringa oleifera* extracts (El-Sayed et al. 2020) and *Mikania micrantha* leaves extracts (Fajar et al. 2020). All these Ag NPs were coated onto cotton fabrics by different techniques and then studied with good results against several common fungi strains. Another approach was based on coating, by pad-dry-cure process, Ag NPs previously formed on siliceous matrixes dopped with carbon including a calcination step (Igal et al. 2019). Furthermore, bimetallic Ag/Cu NPs exhibited a pronounced antimycotic activity (Eremenko et al. 2016; Paszkiewicz et al 2016).

Among nanostructures of metal oxides, ZnO and TiO_2 nanoparticles are the most studied. Gafur and co-workers prepared ZnO NPs and coated them on cotton fabrics using the dip coating technique (Roy et al. 2020). El-Nahhal's group used ultrasound irradiation for the deposition of ZnO NPs on cotton fibers (El-Nahhal et al. 2017). Gowri and collaborators described the obtention of antimicrobial TiO_2 nanoparticles from titanium tetraisopropoxide and extracts derived from *Aloe vera* plant, after calcination at 500 °C (Gowri et al. 2016). In 2019, functional antimicrobial cotton was prepared applying TiO_2 NPs and green walnut shell dye to modify the metal oxide NPs and achieve natural dye coloration (Nazari 2019). Djamaan and collaborators dispersed TiO_2–SiO_2/chitosan NPs on cotton fabrics surface (Rilda et al. 2016). The hybrid TiO_2–SiO_2/chitosan (2:1) NPs presented high ability to generate hydroxyl radicals and the superoxide anion, which can destroy the fungi's cell membranes.

In some cases, mixtures of metal and metal oxide NPs have been used for multifunctional thincoating textile finishing. The use of hybrid Al_2O_3/SiO_2 modified with Ag/Cu NPs and TiO_2 P25 was described in 2017 (Kowalczyk et al 2017). Gao's research group prepared silver/zinc oxide (Ag/ZnO) NPs with different molar ratios by chemical precipitation method observing a synergism between ZnO and Ag NPs in the antimicrobial properties of coated cotton fabrics (Gao et al. 2020).

Considering the mentioned precedents, we envisaged the development of a different approach to achieve modified cotton fabrics with antifungal properties. Taking advantage of the long experience of the group in carrying out sol–gel processes for the preparation of hybrid silicas (Trilla et al. 2009; Bernini et al. 2010; Boffi et al. 2011; Monge-Marcet et al. 2012; Borja et al. 2012); Fernández et al. 2014; Ferré et al. 2016) and in the coating of textiles (Soler et al. 2011; Salabert et al. 2015; Montagut et al. 2017; Montagut et al. 2019a, b; Li et al. 2020a), we envisioned the covalent anchoring of well-known antifungal agents on silica nanoparticles (either dense or mesoporous), which have deserved great attention as a biocompatible form of silica (Tang et al. 2012; Tarn et al. 2013; Croissant et al. 2015; Ni et al. 2018). Miconazole core was chosen as a model structure because it has been traditionally used to topically treat superficial infections caused by fungi. Like other azole antifungals, Miconazole exerts its effect by disrupting the cell membrane of the fungus. Miconazole inhibits ergosterol synthesis by interacting with

14-alpha demethylase, a cytochrome P-450 enzyme that is required for the conversion of lanosterol to ergosterol, an essential membrane component. Inhibition of ergosterol synthesis results in increased cell permeability, causing filtration of cell contents. Miconazole does not have the same effect on human cholesterol synthesis. Other antifungal effects of imidazole derivatives have been proposed that include inhibition of endogenous respiration, interaction with membrane phospholipids, and inhibition of yeast transformation to mycelial forms. Other mechanisms may involve inhibition of uptake and impairment of triglyceride and phospholipid biosynthesis (Sheehan et al. 1999).

For this purpose, the drug must be derivatized by adding a terminal group of the triethoxysilyl type that allows condensation with tetraethoxysilane (TEOS) in the presence of a catalyst. Alternatively, the grafting of the silylated derivatives to previously formed mesoporous silica nanoparticles of MCM-41 type would also be performed. The functionalized non-porous or mesoporous silica nanoparticles would be dispersed onto cotton fabrics surfaces and studied for potential topical anti-fungal applications in medical textiles (bandages, gauzes or strips). Furthermore, the presence of functionalized silica nanoparticles in dressings would increase the roughness of the surface of the fabric and, consequently, its hydrophobicity and durability (Wang et al. 2008; Xue et al. 2009; Zhang et al. 2013). The moisture rejection is advantageous for keeping dry the gauze, acting as a barrier to the microorganisms.

Experimental section

Materials

All chemicals were purchased from Fluorochem and Merck, and they were used without further purification, unless specified. MCM-41 nanoparticles (Li et al. 2020a), (3-iodopropyl)triethoxysilane (Guo et al. 2013) and (3-azidopropyl)triethoxysilane (Li et al. 2019) were prepared as previously reported in our group.

Characterization techniques

The ^{1}H and ^{13}C NMR spectra were recorded at 298.0 K on a Bruker DPX-360 or 400 MHz Bruker Advance-III equipped with a BBFO probe with an automatic tuning. All the spectra were calibrated using the residual solvent signal (CDCl$_3$, δ_H, 7.26 and δ_C, 77.16 ppm and CD$_3$OD, δ_H, 3.31 and δ_C, 49.0 ppm). Chemical shift data were expressed in ppm and coupling constant (J) values in Hz. Multiplicity of peaks was abbreviated as s (singlet), d (doublet), t (triplet), q (quartet), and dd (doublet of doublets). The ^{29}Si and ^{13}C CP-MAS NMR spectra were obtained from a Bruker AV400WB, the repetition time was 5 s with contact times of 2 ms and the number of scans acquired was between 800 and 1600. This NMR instrument belongs to the *Servicio de Resonancia Magnética Nuclear de Sólidos del Instituto de Ciencia de Materiales de Madrid—CSIC*. FTIR spectroscopy was recorded with a Bruker Tensor 27 spectrometer using a Golden Gate ATR module with a diamond window. High resolution mass spectra were obtained by direct injection of the sample with electrospray techniques in Hewlett-Packard 5989A and microTOF-Q instruments, respectively. Elemental analysis of C, N, and H were performed using Flash 2000 Organic Elemental analyzer of Thermo Fisher Scientific with BBOT as an internal standard. Transmission electron microscopy (TEM) analyses were performed on a JEM-2011 Electron Microscope at 200 kV. Scanning electron microscopy (SEM), energy-dispersive X-ray spectroscopy (EDX), and element line scans mapping were taken on a SEM Zeiss Merlin with and INCA detector from Oxford Instruments. Thus, microscopic investigations of the specimens were carried out using a ZEISS MERLIN scanning electron microscope (SEM). The specimens were mounted on conductive carbon adhesive tabs and images were taken after the specimens had been sputter-coated (K550X EMITECH) with a very thin layer of gold. For the elemental composition of the fabric surface, an INCA energy dispersive X-ray (EDX) detector from Oxford Instruments was used. Dynamic light scattering (DLS) and zeta potential measurements have been performed using a Zetasizer Nano ZS (Malvern Instruments) with 8 mg of silica NPs in 8 mL of Milli-Q water, and the pH of the solution was measured by CRISON pH meter Basic 20. The surface areas were determined by the

Brunauer–Emmett–Teller (BET) method from N_2 adsorption–desorption isotherms obtained with a Micromeritics ASAP2000 analyzer after degassing samples for 55 h at 30 °C under vacuum. Powder X-ray diffraction (P-XRD) was performed with X'Pert Power (PANalytical, Almelo, Netherlands), 45 kV/40 mA, Kα 1.5419 Å with a cooper anode. For contact angle (CA) measurements, the hydrophobic tests performed were the measurement of the contact angle of a water droplet (4 μL) deposited on top of each fabric. These experiments were carried out at ICMAB installations with a Contact Angle Measuring System DSA 100 from KRÜSS, which is located in a physico-chemical laboratory (humidity and temperature control).

*General procedure for the preparation of 4-((1-(2,4-dichlorophenyl)-2-(1H-imidazol-1-yl) ethoxy)methyl) arenes (1 (*Chevreuil et al. 2006*), 2 (*Oh et al. 2011*), 5 and 7)*

In a flame dried Schlenck the benzylic alcohol derivative (1 equiv) was dissolved in 10 mL of anhydrous THF under argon atmosphere. Then, sodium hydride (60% in mineral oil, 4 equiv) was added to the solution and the mixture was stirred at rt for 15 min. Then, the corresponding benzylic bromide (1.23 equiv) was added and the mixture was stirred at rt until completion of the reaction (3 h). When the reaction was over, 10 mL of cold water was added, followed by the addition of 20 mL of dichloromethane. The organic phase was separated, and the aqueous layer was extracted with more dichloromethane. The organics were combined, dried over anhydrous sodium sulphate and evaporated under reduced pressure. The products were purified by flash column chromatography (Rf for product **1** = 0.3; Rf for product **2** = 0.28; Rf for product **5** = 0.25; Rf for product **7** = 0.45 (hexane: AcOEt 1:4)).

General procedure for the preparation of imidazolium iodides (*3, 4 and 10*)

A solution of the corresponding imidazole derivative (1 equiv.) and triethoxy(3-iodopropyl)silane (1 equiv.) in dry acetonitrile (20 mL) was refluxed under argon overnight. After completion of the reaction, the solvent was removed under high vacuum. The final oil

was washed with anhydrous pentane, affording the corresponding imidazolium iodide in excellent yield.

Procedure for the preparation of *6*

Step 1: 3-chloro-4-((1-(2,4-dichlorophenyl)-2-(1H-imidazol-1-yl)ethoxy)methyl)benzaldehyde (5a)

To a stirred solution of compound **5** (1 mmol, 0.41 g) in dry toluene at 0 °C was added 1.5 mL of a DIBAL solution in toluene (1 M). The reaction was stirred at 0 °C for 60 min. Afterwards, hydrochloric acid 10 M (10 mL) was added to the mixture, and when the solution turned a white slurry, 20 mL of HCl 1 M was added. Then, a solution of 5% $NaHCO_3$ was added until the pH of the aqueous solution was 10. The organic phase was separated, and the aqueous phase was further extracted with dichloromethane. The organics were combined, dried over anhydrous Na_2SO_4 and the solvent removed under high vacuum. The titled compound **5a** was purified as an oil from the crude by flash column chromatography using hexane:ethyl acetate (1:9) as eluent (Rf = 0.3 (hexane:ethyl acetate (1:9)) (69% yield, 285 mg, 0.69 mmol).

Step 2: (3-chloro-4-((1-(2,4-dichlorophenyl)-2-(1H-imidazol-1-yl)ethoxy)methyl)phenyl)methanol (5b)

To a stirred solution of compound **5a** (2.9 mmol, 1.2 g) in methanol (20 mL) at rt was added in one portion 0.22 g (5.8 mmol) of NaBH4. After 3 h, the methanolic solution was poured into 100 mL of water. The solution was transferred into a separatory funnel, and extractions with dichloromethane were performed. The organics were collected, dried over anhydrous sodium sulphate, and the solvent removed under high vacuum. The titled compound **5b** (0.96 g, 2.35 mmol, 81% yield) was obtained as oil after purification from the crude by flash column chromatography using ethyl acetate as eluent.

Step 3: 3-chloro-4-((1-(2,4-dichlorophenyl)-2-(1H-imidazol-1-yl)ethoxy)methyl)benzyl (3-(triethoxysilyl)propyl)carbamate (6)

To a stirred solution of compound **5b** (0.61 mmol, 250 mg) in dry THF (5 mL) was added triethoxy(3-isocyanatopropyl)silane (0.15 mL, 0.24 mmol) and

0.01 mL of dibutyltin dilaureate. The reaction was led to proceed overnight under reflux. Next, the solvent was evaporated under high vacuum. The crude was purified by flash column chromatography using ethyl acetate as eluent to obtain **6** as a colorless oil (Rf = 0.43 (ethyl acetate) (81% yield, 324 mg, 0.50 mmol).

Procedure for the preparation of *9*

Step 1: 4-(3-chloro-4-((1-(2,4-dichlorophe nyl)-2-(1H-imidazol-1-yl)ethoxy)methyl)phe nyl)-2-methylbut-3-yn-2-ol (8)

Compound **7** (0.50 g, 1.08 mmol) was dissolved in a degassed mixture of 3 mL of water and 3 mL of 1,2-dimethoxyethane under nitrogen atmosphere. To the solution were added K_2CO_3 (375 mg, 2.71 mmol), CuI (8.3 mg, 0.04 mmol), PPh_3 (23 mg, 0.08 mmol) and Pd/C (23 mg, 0.02 mmol). The mixture was stirred for 30 min at rt and then the alcoholic alkyne was added through syringe (0.26 mL, 2.74 mmol). The reaction was stirred overnight at 80 °C under inert atmosphere, then the mixture was cooled to room temperature, filtered through Celite® and extracted with dichloromethane three times. The organics were washed with water, dried, and concentrated in vacuo. The residue was purified by flash column chromatography (AcOEt 100%) to afford **8** as a white solid (Rf = 0.2 (ethyl acetate) (78% yield, 393 mg, 0.84 mmol).

Step 2: 1-(2-((2-chloro-4-ethynylbenzyl) oxy)-2-(2,4-dichlorophenyl)ethyl)-1H-imidazole (8a)

The alcohol **8** (720 mg, 1.44 mmol) was dissolved in dry toluene (30 mL) in a round-bottom flask. Then NaH (60% in mineral oil, 0.6 mg, 0.014 mmol) was added and a distillation system was adapted. The system was heated at 130 °C for 2 h. After this time, the TLC showed full conversion and most of the toluene has been distilled. The crude mixture was directly poured into a flash silica gel column chromatography and eluted with pure AcOEt. Terminal alkyne **8a** was obtained as a colorless solid in 93% yield (586 mg, 1.33 mmol).

Step 3: 4-(3-chloro-4-((1-(2,4-dichloroph enyl)-2-(1H-imidazol-1-yl)ethoxy)methyl) phenyl)-1-(3-(triethoxysilyl)propyl)-1H-1,2,3-triazole (9)

The alkyne **8a** (400 mg, 1.0 mmol) and 3-(azidopropyl)triethoxysilane (0.246 g, 1 mmol) were dissolved in dry acetonitrile (4 mL) in a microwave tube. Then $CuBr(PPh_3)_3$ (9.2 mg, 0.01 mmol) was added and the system was closed. The tube was introduced in the microwave apparatus and the reaction was led to proceed at 120 °C and 200 W for 10 min. Afterwards, the solution was filtered through Celite® and then the solvent was evaporated. The residue was gently washed with dry pentane. The final compound **9** was obtained as a colorless oil in 92% yield (601 mg, 0.92 mmol).

General procedure for the preparation of functionalized silica nanoparticles by co-condensation method (*dN1–dN5*)

Tetraethoxysilane (2.08 g, 10.0 mmol) and the corresponding silylated antifungal (**3**, **4**, **6**, **9** or **10**) (0.75 mmol) were dissolved in absolute EtOH (35 mL). Then, an ammonium hydroxide-ethanol solution was added (9 mL of 28% $NH_3 \cdot H_2O$ in 35 mL EtOH). The mixture was magnetically stirred intensively (1400 rpm) at room temperature for 12 h. The functionalized nanoparticles were collected by centrifugation (12,000 rpm for 10 min) and washed with ethanol until neutral pH was reached. Then, the obtained white solid was washed successively with Milli-Q water and 96% ethanol, and the nanomaterials were dried under high vacuum.

General procedure for the preparation of functionalized silica nanoparticles by grafting method (*mN6–mN8*)

The corresponding silylated antifungal derivative (0.30 mmol) and mesoporous silica nanoparticles of MCM-41 type (360 mg) were refluxed in anhydrous toluene (60 mL) for 24 h in a 250 mL round bottom flask equipped with a Dean-Stark apparatus. Then the suspension was centrifuged (13,500 rpm at 25 °C for 45 min). The solid was washed successively with ethanol (3 × 30 mL), acetone (2 × 30 mL) and dichloromethane (2 × 30 mL) (30 min at 50 °C under

sonication, 30 min for centrifugation), and further dried under high vacuum to give the grafted material as a white solid.

General procedure for the one-step coating of cotton fabrics with antifungal nonporous silica nanoparticles (*Fabric dN1-Fabric dN5*)

Tetraethoxysilane (2.08 g, 10.0 mmol) and the corresponding silylated antifungal (**3**, **4**, **6**, **9** or **10**) (0.75 mmol) were dissolved in absolute EtOH (35 mL). Then, an ammonium hydroxide-ethanol solution was added (9 mL of 28% NH_3 H_2O in 35 mL EtOH). The mixture was magnetically stirred intensively (1400 rpm) at room temperature for 12 h and then ultrasonicated for 30 min. Afterwards, a piece of white clean 100% cotton (3×3 cm) previously washed with soap and sodium carbonate and dried as previously reported in our group (Salabert et al. 2015), was immersed in the prepared coating solution and the whole system was ultrasonicated for 30 min. After this period of time, the cotton fabric was removed from the solution, washed with water several times and dried in a vacuum oven at 50 °C for several hours.

General procedure for the coating of cotton fabrics with antifungal mesoporous silica nanoparticles (*Fabric mN6-Fabric mN8*)

The corresponding silylated antifungal derivative (0.30 mmol) and mesoporous silica nanoparticles of MCM-41 type (360 mg) were refluxed in anhydrous toluene (60 mL) for 24 h in a 250 mL round bottom flask equipped with a Dean-Stark apparatus. The resulting mixture was ultrasonicated for 30 min and then a piece of clean cotton fabric (3×3 cm) was immersed in the prepared coating solution. The whole system was ultrasonicated for 30 min. After this period of time, the cotton fabric was removed from the solution, rinsed with toluene and dried in a vacuum oven at 50 °C for several hours.

Antifungal activity of the modified cotton fabrics

With the coated fabrics with nanoparticles in hand, their effectiveness against four microorganisms (filamentous fungi and yeast) was measured (Trichophyton mentagrophytes CECT 2783, *Aspergillus*

brasiliensis CECT 2091, *Penicillium chrysogenum* CECT 2307 and Candida albicans CECT 1001). A suspension of known concentration was prepared by titration (by preparation of serial dilutions and seeding) of the order of 106 CFU / mL (Colony Forming Units) of each fungal culture. In addition, two assays were performed where sterile Petri dishes were prepared and fragments of the fabrics were deposited (each containing a different type of nanoparticle) and each type of nanoparticle had four replicated impregnated each with one of the four types of fungus. One of the trials was at time 0 and another with a 24-h exposure (during this period they were kept at 25 °C and in aerobiosis). Immediately after impregnating the fabrics, in the time trial 0, the deposited culture was recovered using a sterile swab and reseeded in Petri dishes containing Agar Saboureaud (a suitable culture medium for the correct growth of the fungi). The results of this test correspond to the maximum number of CFU that can be recovered per plate just after the direct contact of the fungi with the studied fabrics. The inoculated plates were kept in an oven for 3–5 days at 25 °C in aerobiosis and then proceed to the reading of CFU developed at time 0 (CFU_0). By contrast, the second group of fabrics was kept in contact with fungi for 24 h. After this time, the same procedure was done as with time group 0, obtaining in this case the CFU in 24 h (CFU_{24}). Once the results were obtained, the effectiveness of the antifungal can be expressed in % effectiveness as $[(CFU_0 - CFU_{24})/CFU_0] \times 100$.

Results and discussion

Synthesis of silylated derivatives of antifungals

As we have mentioned, Miconazole core was chosen as a model structure. In order to covalently attach the antifungal units onto silica nanoparticles, the presence of a triethoxysilyl moiety on its structure was selected. Different linkers to attach this silylated unit were evaluated (such as carbamate and triazole). Additionally, as Miconazole is pharmacologically used as a nitrate salt, the alkylation of the imidazole ring with a silylated alkyl iodide was also considered (Scheme 1).

First, we developed a bimolecular nucleophilic substitution between Miconazole (**1**) and
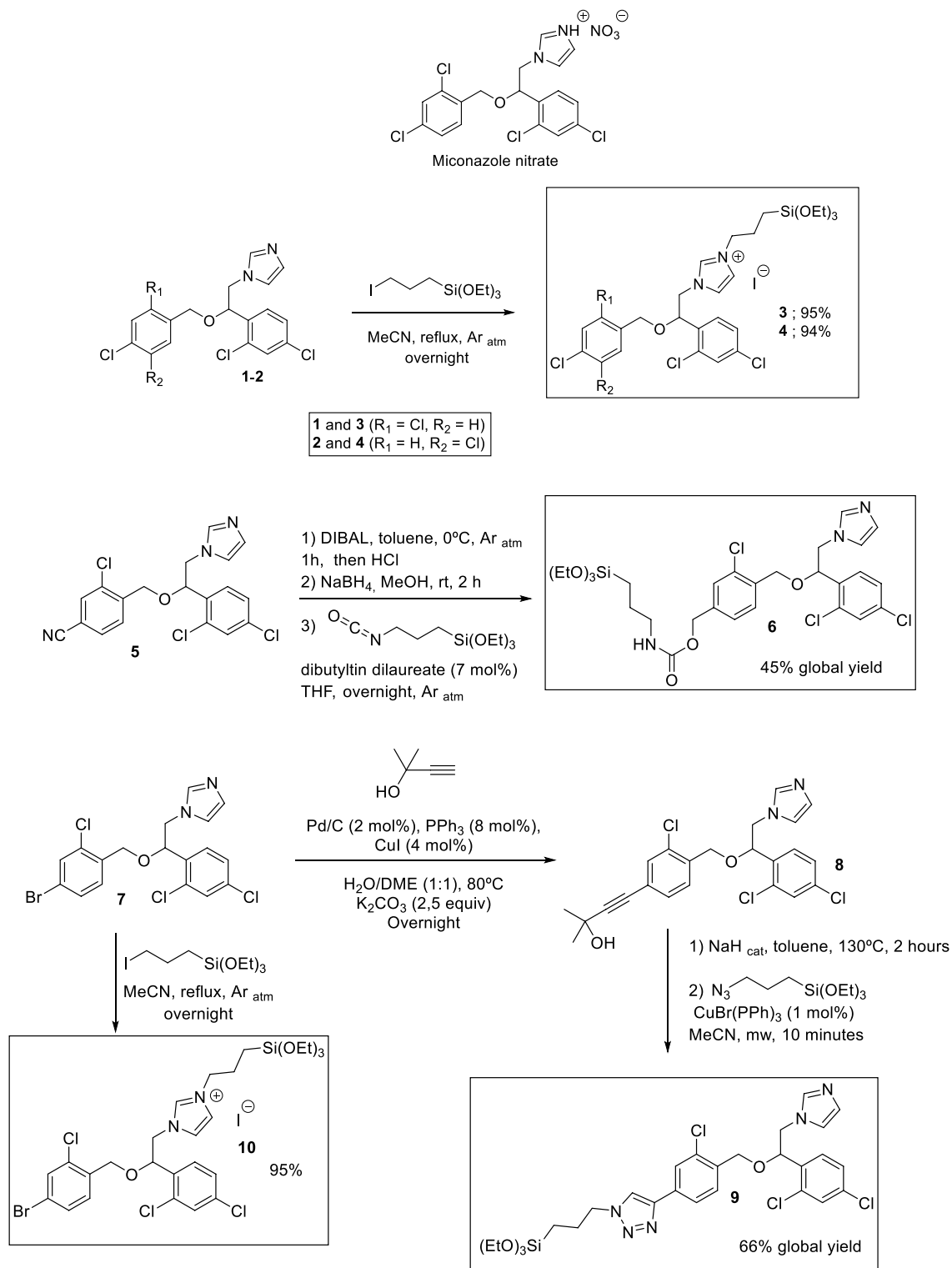
Scheme 1 Synthesis of silylated drug derivatives **3**, **4**, **6**, **9** and **10**

3-iodopropyltriethoxysilane in dry acetonitrile, yielding the corresponding imidazolium iodide **3** (95% yield). As we also wanted to check the importance of the position of the chlorine atoms in the benzyloxy moiety, we prepared the silylated imidazolium iodide **4** from **2** by an analogous procedure (94% yield). Then, we replaced the chlorine atom in position 4 of the aryl ring of the benzyloxy moiety present in Miconazole by a silylated carbamate (**6**) or by a silylated triazole ring (**9**) (Scheme 1).

The preparation of **6** was undertaken from the nitrile **5**. First, the nitrile was reduced to the corresponding aldehyde (69%) by DIBAL at 0 °C in dry toluene. Then, the carbonyl group was reduced to the primary alcohol (81% yield) with sodium borohydride. Finally, the alcohol reacted with the silylated isocyanate efficiently in refluxing THF using dibutyltin dilaureate as catalyst to afford the carbamate **6** (81% yield). Thus, compound **6** was prepared in three steps in 45% overall yield from **5** (Scheme 1). On the other hand, compound **9** was synthesized from the bromoarene **7** through a Sonogashira coupling with 2-methylbut-3-yn-2-ol as a first step, yielding alkyne **8** in a 78% yield. This alkyne was deprotected under catalytic NaH to afford the corresponding terminal alkyne (92% yield), which was coupled with (3-azidopropyl)triethoxysilane giving **9** (92% yield) through a click Cu-catalyzed azide-alkyne Huisgen reaction (Breugst and Reissig 2020; Hettegger et al. 2015b) under microwave and anhydrous conditions (Bürglová et al. 2011). Thus, the silylated triazole derivative **9** was prepared in a 66% global yield in three steps from **7** (Scheme 1). Finally, the silylated imidazolium iodide **10** was prepared from **7** (95% yield) to check the effect of the change of the chlorine by a bromine atom in the antifungal activity (Scheme 1).

Preparation and Characterization of Antifungal-Functionalized Silica Nanoparticles

With the modified silylated antifungal molecules (**3**, **4**, **6**, **9** and **10**, Scheme 1) in hand, we turned to the covalent anchoring of these drugs to silica nanoparticles. We followed two different approaches. First, we prepared nonporous nanomaterials **dN1–dN5** by co-condensation of silylated precursors (**3**, **4**, **6**, **9** or **10**) with TEOS using a 28% aqueous ammonia solution in ethanol (Li et al. 2020a; Wang et al. 2008) (Scheme 2). The mixed solution was stirred at room temperature for 12 h and then the dense nanoparticles were collected by centrifugation (13,500 rpm) and washed successively with ethanol, Milli-Q water, and ethanol until neutral pH.

On the other hand, functionalized mesoporous silica nanoparticles **mN6–mN8** (Scheme 2) were prepared by grafting the corresponding silylated drugs to previously synthesized mesoporous silica nanoparticles of MCM-41 type (Théron et al. 2014) in refluxing toluene for 24 h. The NPs were collected by centrifugation (13,500 rpm) and then washed successively with ethanol, acetone, and dichloromethane.

These nanomaterials were characterized by elemental analysis, transmission electron microscopy (TEM), dynamic light scattering (DLS), zeta-potential, infrared spectroscopy, powder XRD and nitrogen-sorption measurements when appropriate.

In Table 1 are summarized some physical data obtained after characterization. First, the nanometric size and morphology of these materials were analysed by TEM and DLS. Materials **dN1**, **dN2** and **dN3** prepared by co-condensation of silylated imidazolium iodides **3**, **4** and **10** in basic medium in the absence of template appeared as nonporous dense aggregates and they showed high polydispersity in the dynamic light scattering measurements (Table 1).

Contrarily, **dN4** and **dN5** prepared from neutral silylated precursors **6** and **9** under analogous conditions exhibited spherical morphology, with diameters around 136 ± 31 nm and 206 ± 45 nm (see the TEM image of **dN5** in Fig. 1, left, as an example) and showed a good polydispersity index in DLS (Table 1 and Supplementary Information).

Besides, **mN6–mN8** nanomaterials prepared by grafting appeared as mesoporous spherical nanoparticles with average diameters of 86 ± 24, 140 ± 17 and 147 ± 31 nm (see Table 1 and Supplementary Information). A selected TEM image of **mN6** is given in Fig. 1, right). The BET surface area of **mN6** and **mN8** were 313 and 192 m^2 g^{-1}, respectively. The *p*-XRD analyses showed the organized porosity for the MCM-41 materials, typical for a hexagonal 2D symmetry (see Fig. 2 for the *p*-XRD of **mN8**).

In these cases, DLS measurements showed hydrodynamic diameters that are in agreement with the TEM size of the corresponding dried nanoparticles if we consider the likely adsorption of water molecules onto the nanoparticle surface (Table 1). The drug
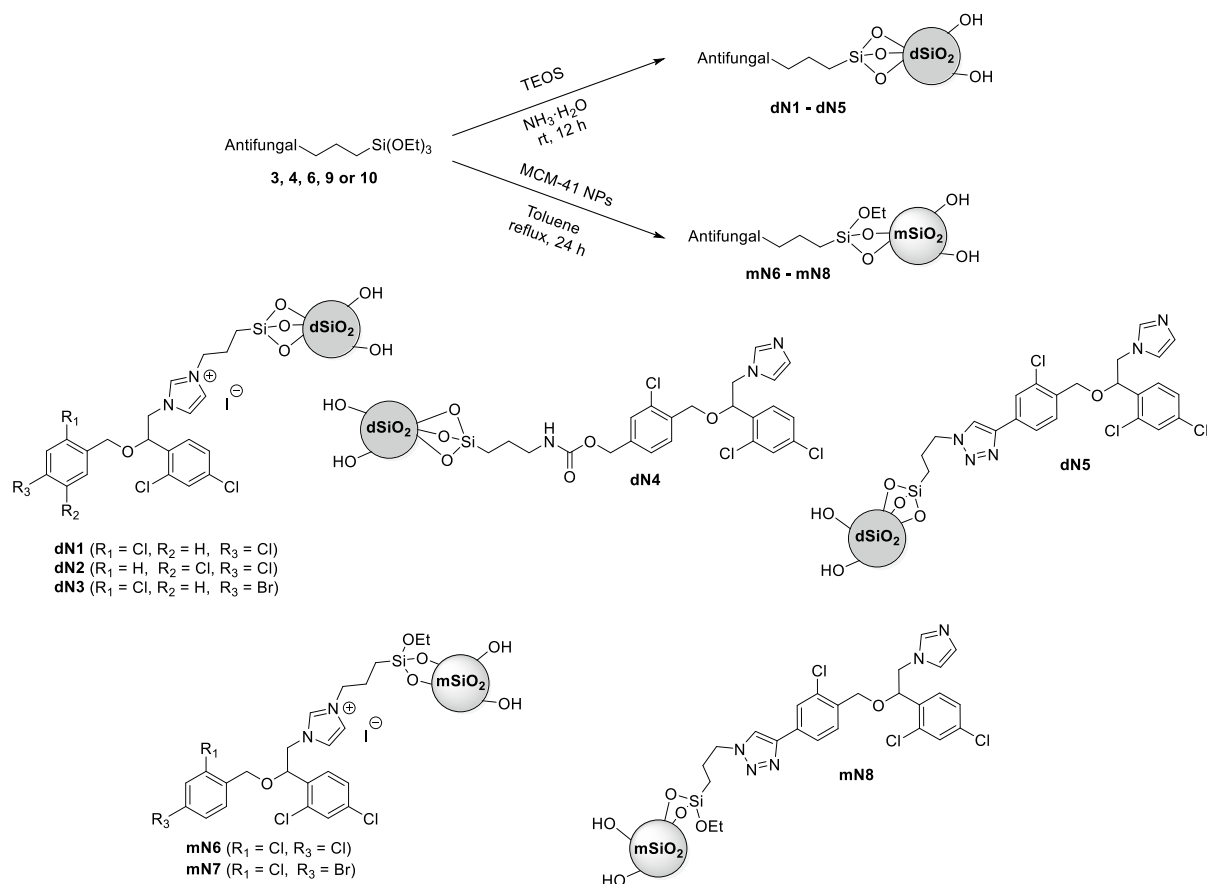
Scheme 2 Preparation of drug functionalized silica nanoparticles

Table 1 Characterization data of **dN1–dN5** and **mN6–mN8**

Material	Drug loading (mmol g^{-1})[a]	Particle size (nm)		Z-potential (mV)
		TEM	DLS[b]	
dN1	0.507	nd[c]	nd[c]	+50.2
dN2	0.332	nd[c]	nd[c]	+37.3
dN3	0.360	nd[c]	nd[c]	+37.4
dN4	0.263	136±31	427	−64.7
dN5	0.244	206±45	416	−21.0
mN6	0.514	86±24	120	+37.0
mN7	0.471	140±17	215	+35.6
mN8	0.377	147±31	204	−28.1

[a]Calculated from the N elemental analysis

[b]Hydrodynamic diameters

[c]Not determined, the sample presented high polydispersity index

loading in the NPs was determined from the nitrogen elemental analysis (Table 1).

The stability of all nanoparticles in milli-Q water suspension (1 mg/mL) was checked by zeta potential. The nanomaterials (**dN1, dN2, dN3, mN6** and **mN7**) prepared from the imidazolium salts presented positive values from +35.6 to +50.2 mV, which are in good agreement with a good stability in water suspension and the presence of cationic imidazolium moieties on the surface of the particles. On the other hand, the nanoparticles (**dN4, dN5** and **mN8**) synthesized from neutral silylated derivatives showed negative zeta potential values (from −21 to −64.7 mV) also indicative of a good stability. The negative sign in these samples is in consonance with the non-protonation of the basic imidazole ring and the residual deprotonated silanol groups.

Solid state ^{29}Si and ^{13}C NMR spectra ensured the presence of the corresponding organic moiety in

Fig. 1 Left: TEM image of **dN5**. Right: TEM image of **mN6**
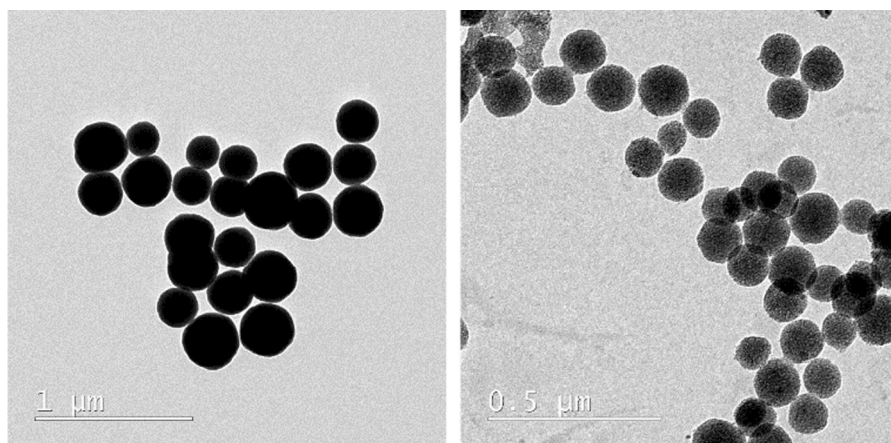
the nanomaterials. The ^{29}Si CP MAS NMR showed two groups of chemical shifts: T units from -61 to -69 ppm formed from the organosilanes and Q units ranging from -90 to -111 ppm resulting from TEOS. The presence of T signals suggested that the integrity of the Si–C bond was maintained during the formation of the nanomaterials, which was also confirmed by a signal between 8 and 10 ppm in the solid state ^{13}C NMR spectra (see the Supplementary Information for the solid-state NMR spectra of the nanoparticles).
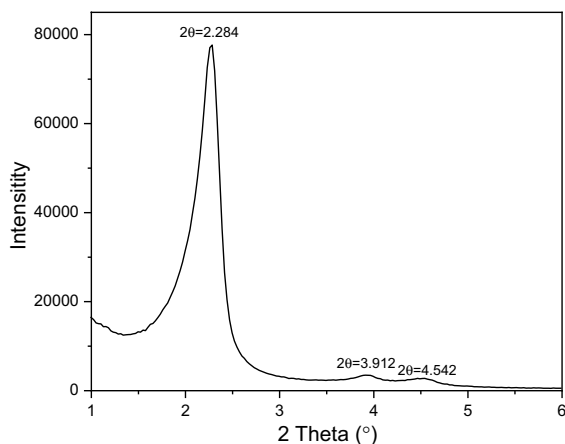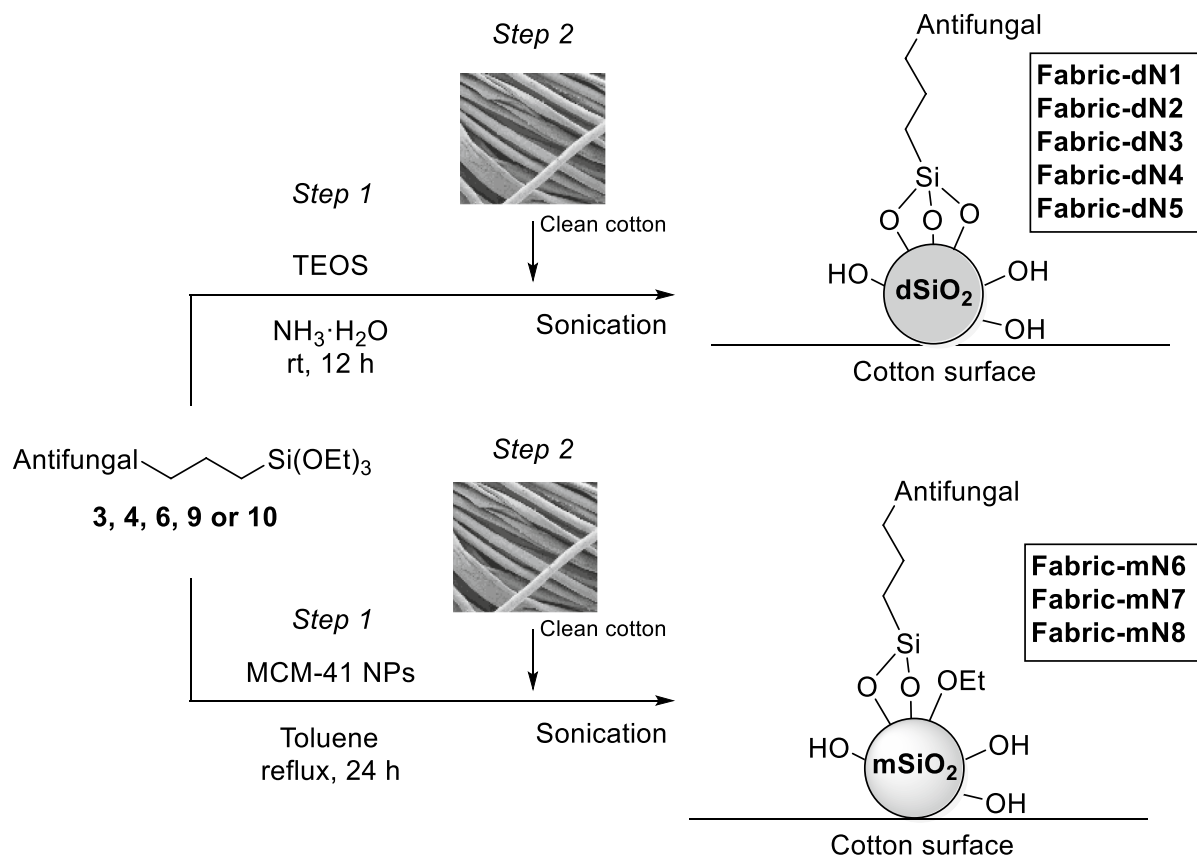

Fig. 2 *p*-XRD of **mN8**

Preparation and characterization of cotton fabrics coated with antifungal-functionalized silica nanoparticles

The preparation of cotton fabrics coated with drug-functionalized silica nanoparticles was performed as represented in Scheme 3. On one hand, once the grafting procedure for the preparation of mesoporous functionalized nanoparticles was finished, a piece of 3×3 cm of clean cotton fabric was immersed into the previously sonicated solution (30 min) and further sonicated for 30 min. After this time, the cellulose material was removed, washed with toluene, and dried under high vacuum at 50 °C.

On the other hand, a piece of 3×3 cm of clean cotton fabric was added to a previously sonicated (30 min) milky solution resulting from the co-hydrolysis of TEOS with organosilanes in aqueous ammonia in ethanol, and further sonicated for 30 min. Afterwards, the cotton fabric was removed from the solution, washed with distilled water, and then dried under high vacuum at 50 °C.

The cotton textiles coated with the nanostructures were analysed by scanning electron microscopy (SEM). In Fig. 3 the SEM image of **Fabric-dN5** is presented (see Supplementary Information for the other modified cotton fabrics). In the SEM image the cotton fabrics appears covered by functionalized

Scheme 3 Preparation of cotton fabrics coated with antifungal-functionalized silica nanoparticles

silica nanoparticles. The surface composition was checked by energy dispersive X-ray spectroscopy (EDX) and element mapping. The presence of Si, C, O, N and in some cases Cl and Br atoms were clearly observed (see Fig. 3 for the element mapping for **Fabric-dN5** and the Supplementary Information for the other modified textiles). The cotton fabrics (**Fabric-dN1**–**Fabric-dN3**) coated with dense nonporous nanoparticles prepared from silylated imidazolium iodides presented cauliflower like structures, in agreement with the high polydispersity index observed in the DLS measurements of the corresponding nanoparticles (**dN1**-**dN3**). On the contrary, cotton fabrics (**Fabric-dN4** and **Fabric-dN5**) coated with dense nanoparticles prepared from the non-charged imidazole-containing organosilanes presented high homogeneity regarding the particles size. This last feature was also observed in cotton fabrics (**Fabric-mN6**–**Fabric-mN8**) coated with functionalized mesoporous nanoparticles, regardless of the chemical

nature of the employed organosilane. The measured contact angle for **Fabric-dN3** and **Fabric-dN5** were 131 and 148°, respectively, indicative of hydrophobic surfaces. Contrarily, **Fabric-mN7** and **Fabric-mN8** were not hydrophobic as the water drop was absorbed by the modified fabrics after a few seconds.

Antifungal activity of the fabrics coated with anti-fungal-functionalized silica nanoparticles

The antifungal activity of all the fabrics coated with antifungal-functionalized silica nanoparticles was tested against four different microorganisms, three filamentous fungi and a yeast (*Trichophyton mentagrophytes CECT 2783*, *Aspergillus brasiliensis CECT 2091*, *Penicillium chrysogenum CECT 2307* and *Candida albicans CECT 1001*). *Trichophyton mentagrophytes* is a fungus which causes ringworm in companion animals, tinea infections in humans and one of the most common fungi that cause zoonotic
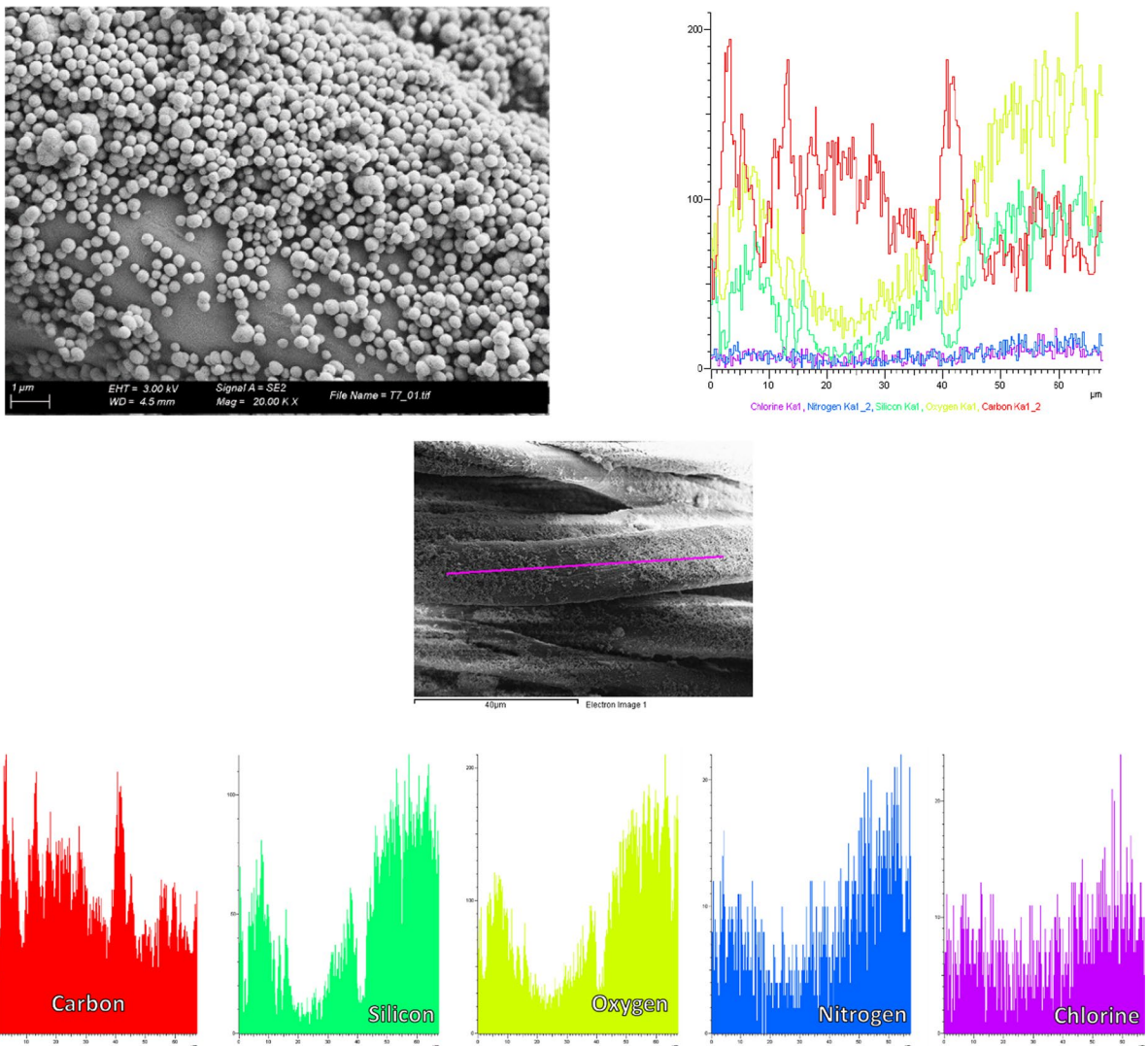
Fig. 3 Left: SEM image of **Fabric-dN5**. Right: Element Mapping of **Fabric-dN5**

skin disease. *Aspergillus brasiliensis* is a major environmental pollutant. *Penicillium chrysogenum* can induce respiratory allergic symptoms such as allergic rhinitis, asthma and allergic broncho-pulmonary mycosis. *Candida albicans* is an opportunistic pathogenic yeast that is a common member of the human gut flora but can cause infections in humans and animals such as candidiasis and onychomycosis.

Preliminary experiments were carried out following the antibiogram technique (antifungigram) (Serrano et al 2004; Ramírez et al 2006; Espinel-Ingroff et al 2007; Martos et al 2012; Colosi et al. 2012) to study the production of inhibition halos using

fragments of the impregnated cotton fabrics (**Fabric-dN2** and **Fabric-dN3**) and confronting them with the fungal strains.

Small pieces of the cotton fabrics were deposited on the surface's plate and inoculated with each of the microorganisms. They were incubated for 24–48 h and the inhibition halos were observed (see Supporting information). Considering these initial positive results, then we carried out a quantitative study of the activity of these impregnated fabrics, mimicking its application on the surface of the skin of the affected organism. The methodology used was a modification of that indicated in international standards (UNE

Table 2 Antifungal activity (% effectiveness) of **Fabrics-dN1** to **Fabric-dN5** and **Fabrics-mN6 to Fabric-mN8**

Material	Strain			
	Trichophyton mentagrophytes	*Aspergillus brasiliensis*	*Penicillium chrysogenum*	*Candida albicans*
Fabric-dN1	90	10	90	55
Fabric-dN2	25	25	0	25
Fabric-dN3	25	25	0	25
Fabric-dN4	90	0	25	25
Fabric-dN5	25	25	0	25
Fabric-mN6	90	10	90	55
Fabric-mN7	90	90	90	75
Fabric-mN8	90	0	25	25

EN ISO 846:2020 Plastics- Evaluation of the action of microorganisms (ISO 846:2019)) to quantify the capacity to reduce the viability of the fungal strains tested. Thus, the modified fabrics were impregnated with the corresponding strain and kept in the stove at 25 oC in aerobiosis for 24 h. The results are shown in Table 2. The activity of the modified fabric has been expressed in % effectiveness as $[(CFU_0-CFU_{24})/CFU_0] \times 100$, where CFU_{24} is the number of fungal cells that are viable after the fabric is kept in contact with fungi for 24 h and CFU_0 is the number of viable fungal cells at time 0 (CFU = Colony Forming Units). To our delight, all the fabrics were found to be moderately (25%) or highly active (90%) against *Trichophyton mentagrophytes.* The effectiveness against the yeast *Candida albicans* varies from 25 to 75%. Whereas **Fabric-dN4** and **Fabric-mN8** were not active against *Aspergillus brasiliensis*, the other modified cotton fabrics exhibited low (10%), moderate (25%) or high (90%) activity. Excellent antifungal properties (90% effectiveness) were found for **Fabric-dN1**, **Fabric-mN6** and **Fabric-mN7** against *Penicillium chrysogenum,* and moderate activity (25%) in the case of **Fabric-dN4** and **Fabric-mN8**. Thus, the antifungal activity of the coated fabrics was found to be highly dependent on the microorganism. That

allows specific fungal treatments for each microorganism. Within the same fungal or yeast strain, some influence of the structural features of the organic moiety or the type of nanoparticles was also observed, although no clear general rule can be inferred from the results. Within *Trichophyton mentagrophytes* the higher % effectiveness of **Fabric-mN7** over **Fabric-dN3** and of **Fabric-mN8** over **Fabric-dN5** (see Table 2) could be attributed to the differences in the hydrophilicity/hydrophobicity of the corresponding surfaces. As the microorganisms are grown in aqueous medium, a hydrophobic antifungal cotton surface would make more difficult the interaction with the fungus. It is noteworthy that **Fabric-dN1**, **Fabric-mN6** and **Fabric-mN7** are good candidates to be used as topical antifungal agents in cotton medical textiles for the remarkable results.

Conclusions

In summary, several silylated derivatives have been prepared taking the topical antifungal agent Miconazole as a model. Different linkers to attach the silylated unit have been employed (carbamate and triazole). Additionally, as Miconazole is used as a nitrate salt, the alkylation of the imidazole ring with a silylated alkyl iodide has also been performed. The covalent anchoring of these silylated derivatives to mesoporous or dense silica nanoparticles has been achieved by grafting and co-condensation procedures, respectively. Furthermore, cotton textiles have been coated with these antifungal-functionalized silica nanoparticles under ultrasonic conditions. The characterization of the functionalized nanoparticles and coated cotton fabrics has been carried out by microscopic and spectroscopic techniques. The antifungal activity of all the modified fabrics has been tested against three filamentous fungi and a yeast (*Trichophyton mentagrophytes CECT 2783*, *Aspergillus brasiliensis CECT 2091*, *Penicillium chrysogenum CECT 2307* and *Candida albicans CECT 1001*) and has been found to be highly dependent on the microorganism. Some influence of the structural features of the organic moiety, the type of nanoparticles and the hydrophobicity of the cotton surface has been also observed, although no general rule can be deduced. Remarkably, all of them have shown activity against *Candida albicans* and *Trichophyton mentagrophytes,*

with up to 75 and 90% effectiveness, respectively, being **Fabric-dN1**, **Fabric-mN6** and **Fabric-mN7** the best candidates to combat general fungal growth. High expectations arise for topical cutaneous applications in wound dressings (bandages, gauzes, strips).

Declarations

References

Ahmed HB, Abualnaja KM, Ghareeb RY, Ibrahim AA, Abdelsalam NR, Emam HE (2021) Technical textiles modified with immobilized carbon dots synthesized with infrared assistance. J Colloid Interface Sci 604:15–29

Almeida F, Rodrigues ML, Coelho C (2019) The still underestimated problem of fungal diseases worldwide. Front Microbiol 10:214

AnwarKhalid Y, Alghamdi M (2020) Imparting antibacterial, antifungal and catalytic properties to cotton cloth surface via green route. Polym Test 81:106258

Bernini R, Cacchi S, Fabrizi G, Forte G, Petrucci F, Prastaro A, Niembro S, Shafir A, Vallribera A (2010) Perfluorotagged, phosphine-free palladium nanoparticles supported on silica gel: application to alkynylation of aryl halides, Suzuki–Miyaura cross-coupling, and Heck reactions under aerobic conditions. Green Chem 12:150–158

Boffi A, Cacchi S, Ceci P, Cirilli R, Fabrizi G, Prastaro A, Niembro S, Shafir A, Vallribera A (2011) The Heck reaction of allylic alcohols catalyzed by palladium nanoparticles in water: chemoenzymatic synthesis of (R)-(-)-Rhododendrol. ChemCatChem 3:347–353

Borja G, Monge-Marcet A, Pleixats R, Parella T, Cattoën X, Wong Chi Man M (2012) Recyclable hybrid silica-based catalysts derived from Pd–NHC complexes for Suzuki, Heck and Sonogashira reactions. Eur J Org Chem 19:3625–3635

Breugst M, Reissig H-U (2020) The Huisgen reaction: milestones of the 1,3-dipolar cycloaddition. Angew Chem Int Ed 59:12293–12307

Brown GD, Denning DW, Gow NAR, Levitz SM, Netea MG, White C (2012) Hidden killers: human fungal infections. Sci Transl Med 4:165rv13

Bürglová K, Moitra N, Hodacová J, Cattoën X, Wong Chi Man M (2011) Click approaches to functional water-sensitive organotriethoxysilanes. J Org Chem 76:7326–7333

Chevreuil F, Landreau A, Seraphin D, Larcher G, Bouchara GP, Richomme P (2006) Synthesis and antifungal activity of new thienyl and aryl conazoles. J Enzy Inhib Med Chem 21:293–303

Colosi IA, Faure O, Dessaigne B, Bourdon C, Lebeau B, Colosi HA, Pelloux H (2012) Susceptibility of 100 filamentous fungi: comparison of two diffusion methods, Neo-Sensitabs and E-test, for amphotericin B, caspofungin, itraconazole, voriconazole and posaconazole. Med Mycol 50:378–385

Croissant JG, Cattoën X, Wong Chi Man M, Durand JO, Khashab NM (2015) Synthesis and applications of periodic mesoporous organosilica nanoparticles. Nanoscale 7:20318–20334

Dawoud TM, Yassin MA, El-Samawaty ARM, Elgorban AM (2020) Silver nanoparticles synthesized by nigrospora oryzae showed antifungal activity. Saudi J Biol Sci 12:36–41

Eid AM, Fouda A, Niedbala G, Hassan SE-D, Salem SS, Abdo AM, Hetta HF, Shaheen TI (2020) Endophytic streptomyces laurentii mediated green synthesis of Ag-NPs with antibacterial and anticancer properties for developing functional textile fabric properties. Antibiotics 9:641–659

El-Nahhal IM, Elmanama AA, El Ashgar NM, Amara N, Selmane M, Chehimi MM (2017) Stabilization of nanostructured ZnO particles onto the surface of cotton fibers using different surfactants and their antimicrobial activity. Ultrason Sonochem 38:478–487

El-Sayed AA, Amr A, Kamel OMHM, El-Saidi MMT, Ahmed E, Abdelhamid AE (2020) Eco-friendly fabric modification based on AgNPs@Moringa for mosquito repellent applications. Cellulose 27:8429–8442

Emam HE, El-Shahat M, Hasanin MS, Ahmed HB (2021) Potential military cotton textiles composed of carbon quantum dots clustered from 4–(2,4–dichlorophenyl)–6–oxo–2–thioxohexahydropyrimidine–5–carbonitrile. Cellulose 28:9991–10011

Eremenko AM, Petrik IS, Smirnova NP, Rudenko AV, Marikvas YS (2016) Antibacterial and antimycotic activity of cotton fabrics, impregnated with silver and binary silver/copper nanoparticles. Nanoscale Res Lett 11:1–9

Espinel-Ingroff A, Cantón E, Gibbs D, Wang A (2007) Comparison of Neo. Sensitabs tablet diffusion assay results on three different agar media with CLSI broth microdilution M27–A2 and M44-A results for testing susceptibility of *Candida* spp and *Cryptococcus neoformans* to amphotericin B, caspofungin itraconazole and voriconazole. J Clin Microbiol 45:858–864

Fajar MN, Endarko E, Rubiyanto A, Malek NANN, Hadibarata T, Syafiuddin A (2020) A green method for the enhancement of antifungal properties of various textiles functionalized with silver nanoparticles. Biointerface Res Appl Chem 10:4902–4907

Fernández M, Ferré M, Pla-Quintana A, Parella T, Pleixats R, Roglans A (2014) Rhodium-NHC hybrid silica materials as recyclable catalysts for [2+2+2] cycloaddition reactions of alkynes. Eur J Org Chem 28:6242–6251

Ferré M, Cattoën X, Wong Chi Man M, Pleixats R (2016) Sol-gel immobilized N-heterocyclic carbene gold complex as a recyclable catalyst for the rearrangement of allylic esters and the cy-cloisomerization of γ-alkynoic acids. ChemCatChem 8:2824–2831

Gao D, Liu J, Lyu L, Li Y, Ma J, Baig W (2020) Construct the multi-function of cotton fabric by synergism between nano ZnO and Ag. Fiber Polym 21:505–512

Garcia-Solache MA, Casadevall A (2010) Global warming will bring new fungal diseases for mammals. Mbio 1:e00061-10

Gargoubi S, Saghrouni F, Chevallier P, Tolouei R, Boudokhane C, Ladhari N, Mantovani D (2020) Polydopamine-modified interface improves the immobilization of natural bioactive-dye onto textile and enhances antifungal activity. Biointerphases 15:041011

Getahun H, Beyer P, Paulin S, Jung L, Huttner B, Ford N (2020) First meeting of the WHO antifungal expert group on identifying priority fungal pathogens. Meeting report. World Health Organization (WHO). https://www.who.int/publications/i/item/9789240006355

Gowri S, Gandhi RR, Senthil S, Suresh J, Sundrarajan M (2016) Enhancing antimicrobial activity of biotemplated TiO$_2$ nanoparticles using aloe vera plant extract. J Bionanosci 10:181–190

Guo W, Monge-Marcet A, Cattoën X, Shafir A, Pleixats R (2013) Sol–gel immobilized aryl iodides for the catalytic oxidative α-tosyloxylation of ketones. React Funct Polym 73:192–199

Hedayatia N, Montazer M, Mahmoudirad M, Toliyat T (2020) Ketoconazole and ketoconazole/β-cyclodextrin performance on cotton wound dressing as fungal skin treatment. Carbohydr Poly 240:116267

Hettegger H, Gorfer M, Sortino S, Fraix A, Bandian D, Rohrer C, Harreither W, Potthast A, Rosenau T (2015a) Synthesis, characterization and photo-bactericidal activity of silanized xanthene-modified bacterial cellulose membranes. Cellulose 22:3291–3304

Hettegger H, Sumerskii I, Sortino S, Potthast A, Rosenau T (2015b) Silane meets click chemistry: towards the functionalization of wet bacterial cellulose sheets. Chemsuschem 8:680–687

Igal K, Arreche R, Sambeth J, Bellotti N, Vega-Baudrit J, Redondo-Gómez C, Vázquez P (2019) Antifungal activity of cotton fabrics finished modified silica-silver carbon-based hybrid nanoparticles. Text Res J 89:825–833

Jabar JM, Alabi KA, Lawal AK (2020) Synthesis, characterization and application of novel 1, 3-bis[(furan-2-yl)methylene]thiourea functional dye on wool and cotton fabrics. SN Appl Sci 2:1850

Kowalczyk D, Brzezinski S, Kaminska I (2017) Multifunctional nanocoating finishing of polyester/cotton woven fabric by the sol–gel method. Text Res J 88:946–956

Li H, Pérez-Trujillo M, Cattoën X, Pleixats R (2019) Recyclable mesoporous organosilica nanoparticles derived from proline-valinol amides for asymmetric organocatalysis. ACS Sustain Chem Eng 7:14815–14828

Li H, Granados A, Fernández E, Pleixats R, Vallribera A (2020a) Anti-inflammatory cotton fabrics and silica nanoparticles with potential topical medical applications. ACS Appl Mater Interfaces 12:25658–25675

Li L, Jung J, Ma W, Wen J, Rena X, Sun Y (2020b) Enhanced antimicrobial and antifungal property of two-dimensional fibrous material assembled by *N*-halamine polymeric electrolytes. Mater Sci Eng C 115:11112

Lim SH, Hudson SM (2004) Application of a fiber-reactive chitosan derivative to cotton fabric as an antimicrobial textile finish. Carbohydr Polym 56:227–234

Martos AI, Martín-Mazuelos E, Romero A, Serrano C, González T, Almeida C, Puchea B, Cantón E, Pemán J, Espinel-Ingroff A (2012) Evaluation of disk diffusion method compared to broth microdilution for antifungal susceptibility testing of 3 echinocandins against *Aspergillus* spp. Diagn Microbiol Infect Dis 73:53–56

Monge-Marcet A, Cattoën X, Alonso DA, Nájera C, Wong Chi Man M, Pleixats R (2012) Recyclable silica-supported prolinamide organocatalyst for direct asymmetric aldol reaction in water. Green Chem 14:1601–1610

Montagut AM, Gálvez E, Shafir A, Sebastián RM, Vallribera A (2017) Triarylmethane dyes for artificial repellent cotton fibers. Chem Eur J 23:3810–3814

Montagut AM, Granados A, Ballesteros A, Pleixats R, Llagostera M, Cortés P, Sebastián RM, Vallribera A (2019a) Antibiotic protected silver nanoparticles for microbicidal cotton. Tetrahedron 75:102–108

Montagut AM, Granados A, Lazurko C, El-Khoury A, Suuronen EJ, Alarcon EI, Sebastián RM, Vallribera A (2019b) Triazine mediated covalent antibiotic grafting on cotton fabrics as a modular approach for developing antimicrobial barriers. Cellulose 26:7495–7505

Nabipour H, Wang X, Rahman MZ, Song L, Hu Y (2020) An environmentally friendly approach to fabricating flame retardant, antibacterial and antifungal cotton fabrics via self-assembly of guanazole-metal complex. J Clean Prod 273:122832

Nazari A (2019) Superior self-cleaning and antimicrobial properties on cotton fabrics using nano titanium dioxide along with green walnut shell dye. Fiber Polym 20:2503–2509

Ni D, Jiang D, Ehlerding EB, Huang P, Cai W (2018) Radiolabeling silica-based nanoparticles via coordination chemistry: basic principles, strategies, and applications. Acc Chem Res 51:778–788

Oh K, Higashi M, Yoshizawa Y (2011) Biological evaluation of imidazole derivatives as inhibitors of hydroperoxide

lyase, a key enzyme in plant volatile biosynthesis. J Pestic Sci 36:58–62

Paszkiewicz M, Golabiewska A, Rajski A, Kowal E, Sajdak A, Zaleska-Medynska A (2016) The antibacterial and antifungal textile properties functionalized by bimetallic nanoparticles of Ag/Cu with different structures. J Nanomater 2016:1–13. https://doi.org/10.1155/2016/6056980

Ramírez M, Serrano MC, Castro C, López E, Almeida C, Martín-Mazuelos E (2006) Comparative study of disc diffusion and microdilution methods in susceptibility testing of micafungin against *Candida* species. J Antimicrob Chemother 58:861–863

Rilda Y, Mahardika G, Alif A, Agustien A, Dachriyanus DA, Djamaan A (2016) Antifungal property of cotton fabric textile: modification of cotton fiber functions by coating compounds of TiO_2–SiO_2/chitosan. Der Pharma Chem 8:124–131

Roy TS, Shamim SUD, Rahman MK, Ahmed F, Gafur MA (2020) The development of ZnO nanoparticle coated cotton fabrics for antifungal and antibacterial applications. Mater Sci Appl 11:601–610

Sahayaraj K, Rajesh S, Rathi JAM, Kumar V (2019) Green preparation of seaweed-based silver nano-liquid for cotton pathogenic fungi management. IET Nanobiotechnol 13:219–225

Salabert J, Sebastián RM, Vallribera A (2015) Anthraquinone dyes for superhydrophobic cotton. Chem Commun 51:14251–14254

Serrano MC, Ramírez M, Morilla D, Valverde A, Chávez M, Martín-Mazuelos E (2004) A comparative study of the disc diffusion method with the broth microdilution and Etest methods for voriconazole susceptibility testing of *Aspergillus* spp. J Antimicrob Chemother 53:739–742

Sheehan DJ, Hitchcock CA, Sibley CM (1999) Current and emerging azole antifungal agents. Clin Microbiol Rev 12:40–79

Soler R, Salabert J, Sebastián RM, Vallribera A, Roma N, Ricart S, Molins E (2011) Highly hydrophobic polyfluorinated azo dyes grafted on surfaces. Chem Commun 47:2889–2891

Tang F, Li L, Chen D (2012) Mesoporous silica nanoparticles: synthesis, biocompatibility and drug delivery. Adv Mater 24:1504–1534

Tarn D, Ashley CE, Xue M, Carnes EC, Zink JI, Brinker CJ (2013) Mesoporous silica nanoparticle nanocarriers: biofunctionality and biocompatibility. Acc Chem Res 46:792–802

Théron C, Gallud A, Carcel C, Gary-Bobo M, Maynadier M, Garcia M, Lu J, Tamanoi F, Zink JI, Wong Chi Man M (2014) Hybrid mesoporous silica nanoparticles with pH-operated and complementary H-bonding caps as an autonomous drug-delivery system. Chem Eur J 20:9372–9380

Trilla M, Pleixats R, Wong Chi Man M, Bied C (2009) Organic-inorganic hybrid silica materials containing imidazolium and dihydroimidazolium salts as recyclable organocatalysts for Knoevenagel condensations. Green Chem 11:1815–1820

Tzhayik O, Lipovsky A, Gedanken A (2017) Sonochemical fabrication of edible fragrant antimicrobial nano coating on textiles and polypropylene cups. Ultrason Sonochem 38:614–621

Wang H, Fang J, Cheng T, Ding J, Qu L, Dai L, Wang X, Lin T (2008) One-step coating of fluoro-containing silica nanoparticles for universal generation of surface superhydrophobicity. Chem Commun 7:877–879

Xue CH, Jia ST, Zhang J, Tian LQ (2009) Superhydrophobic surfaces on cotton textiles by complex coating of silica nanoparticles and hydrophobization. Thin Solid Films 517:4593–4598

Zhang J, Li B, Wu L, Wang A (2013) Facile preparation of durable and robust superhydrophobic textiles by dip coating in nanocomposite solution of organosilanes. Chem Commun 49:11509–11511